SAND2007-0801C

5th US Combustion Meeting
Organized by the Western States Section of the Combustion Institute
and Hosted by the University of California at San Diego
March 25-28, 2007.

Association Kinetics of the $C_3H_3 + C_3H_3$ reaction

Yuri Georgievskii[1]*, Stephen J. Klippenstein*[2]*, and James A. Miller*[1]

[1]*Combustion Research Facility,*
Sandia National Laboratories, Livermore CA 94551-0969, USA

[2]*Chemistry Division,*
Argonne National Laboratory, Argonne, IL, 60439, USA

Reactions between two resonance stabilized free radicals play an important role in the gas phase chemistry leading to the formation of polycyclic aromatic hydrocarbons and soot in flames burning aliphatic fuels. The theoretical prediction of rate coefficients and product distributions for such reactions is complicated by the fact that the initial complex-formation steps and some dissociation steps are usually barrierless. In this paper, direct variable reaction coordinate transition state theory (VRC-TST) is used to accurately predict the combination kinetics of two propargyl radicals. A set of multifaceted dividing surfaces is used to take into account the multiple possible channels of the $C_3H_3 + C_3H_3$ reaction. Because of the resonant nature of the reactants their geometric relaxation appears to be important and is calculated for each mutual orientation of the fragments using UB3LYP/cc-pvdz method. The final energy calculations are performed with the CASPT2(10e,10o)/cc-pvdz method. We have also used the VRC- TST approach to calculate the association rate constant and the corresponding number of states for the $C_6H_5 + H \rightarrow C_6H_6$ exit channel, which is also barrierless. To this end we have used the CASPT2(2e,2o)/cc-pvdz quantum chemistry method with a one-dimensional CAS+1+2+QC/aug-cc-pvtz correction based on a $CH_3 + H$ reference system. The energy and angular momentum resolved numbers of states for the entrance and $C_6H_5 + H$ exit channels obtained with the VRC-TST approach are used in the related master equation calculation to determine the temperature and pressure dependence of the phenomenological rate coefficients. The total rate constant obtained for the $C_3H_3 + C_3H_3$ reaction compares favorably with the experimental data available.

1 Introduction

The recombination reaction of propargyl radicals,

$$C_3H_3 + C_3H_3 \rightarrow \mathrm{Products} \tag{1}$$

is believed to be a critical step in the formation of soot in flames of aliphatic fuels. It leads to the formation of the first aromatic ring, which is considered by some researchers to be the rate-limiting step in the formation of polycyclic aromatic compounds and, ulitmately, in soot formation. Reaction (1) also may serve as a prototype reaction between resonance stabilized radicals important for formation of polycyclic aromatic hydrocarbons.

Reaction (1) is complex. After association of the reactants into a C_6H_6 reactive complex, this complex is subject to multiple transitions between different isomeric forms, of which the most stable is benzene. Some of these isomers can be stabilized by non-reactive collisions or they can dissociate back to reactants or into bimolecular products, $\mathrm{C_6H_5 + H}$ and $\mathrm{C_6H_4 + H_2}$.

To describe the kinetics of such complex reactions and to predict the phenomenological rate coefficients of transformations between different species one should solve a time-dependent, multiple-well master equation (ME). In the framework of the ME methodology the transitions between different species are usually described using transition state theory. Most of these transitions are characterized by potential barriers that separate different isomers and/or bimolecular products. In such situations conventional transition state theory, employing simple rigid-rotor harmonic-oscillator models, can be used to calculate the transition rate constant and the corresponding number of states. On the other hand, the transitions corresponding to some of the entrance and exit channels can be barrierless. For Reaction (1) such barrrierless channels correspond to all three entrance channels and the $\mathrm{benzene} \rightarrow \mathrm{C_6H_5 + H}$ exit channel,

$$\mathrm{C_3H_3 + C_3H_3 \rightarrow CH_2CCHCHCCH_2}, \quad (2)$$

$$\mathrm{C_3H_3 + C_3H_3 \rightarrow CH_2CCHCH_2CCH}, \quad (3)$$

$$\mathrm{C_3H_3 + C_3H_3 \rightarrow CHCCH_2CH_2CCH}, \quad (4)$$

$$\mathrm{benzene \rightarrow C_6H_5 + H}. \quad (5)$$

For barrierless reactions the transition state is not well defined. The separation between the reactants in the transition state can change from 5 to 10 bohr depending on the total energy/temperature of the reaction. As the transition state shifts to smaller separation between the reactants the transitional modes are transformed from hindered rotations to anharmonic vibrations.

Variable reaction coordinate transition state theory (VRC-TST) [1–4] provides an efficient procedure to treat the kinetics of barrierless reactions. In earlier studies [5, 6] we have shown that VRC-TST in conjunction with state-of-the-art electronic structure methods allows one to predict the rate constants with quantitative accuracy for barrierless reactions between different alkyl radicals and the hydrogen atom.

In this paper we apply the VRC-TST methodology to the association reactions (2-5). In recent studies [7, 8] we have developed a new potential energy surface for Reaction (1) built on an earlier work [9, 10] and applied this surface to study Reaction (1) using the ME methodology. In those previous studies analytical model potentials were used for barrierless channels (2-5). In this paper we use the number of states calculated using the VRC-TST method for barrierless channels (2-5) together with the potential energy surface from Ref. [8] to calculate the phenomenological rate coefficients for Reaction (1).

The outline of the paper is as follows. In Section II the computational methods used are described briefly. The results of association kinetics as well as of the master equation calculations are presented in Section III and some general conclusions are given in Section IV.

2 Computational Methodology

2.1 Electronic Structure Methods

Our method of choice for direct potential energy calculations is a complete active space (CAS), second-order perturbation theory (PT2) with a relatively small Dunning-style, double-ζ basis set (cc-pvdz). This method, while correctly treating the inherently multi-reference character of the wave function for radical-radical reactions, compares favorably with the multi-reference configurational interaction method in terms of computational efficiency. At large separations it correctly reproduces the dispersion interaction between the reactants. As was shown in our previous studies [5, 6], inclusion of one-dimensional corrections obtained with a large aug-cc-pvtz basis set yields potential energies accurate enough for quantitative kinetic estimates. The MOLPRO program package [11] was used for all CASPT2 [12] calculations.

In contrast with radicals such as methyl or vinyl, that are not resonance stabilized, we have found that the small two-electron, two-orbital (2e,2o) active space is not sufficient to reproduce the electronic structure of the resonance stabilized radicals correctly. For example, if a (1e,1o) active space is used for an isolated allyl radical with a small deviation from an equlibrium geometry, its doubly-occupied π-orbital tends to localize, providing one double and one single bond between the carbon atoms instead of a delocalized orbital. This behavior leads to discontinuities in the potential. To remedy this problem one must include the affected π-orbitals in the active space. Unfortunately, doing so required that we include the whole π-stack for Reactions (2-4) into our calculation. Thus, a (10e,10o) active space is used in our calculations.

Another peculiarity of reactions between resonance stabilized radicals is related to the fact that the geometry of the reactants changes considerably in the process of chemical bond formation. This feature is related to a considerable change in the electronic structure of the resonance stabilized radicals when a chemical bond is formed. As a result the geometry relaxation of the fragments (conserved mode relaxation) must be incorporated into the calculations to reproduce correctly the effective interaction potential between the fragments. In Fig. 1 the effect of the geometry relaxation on the interaction energy is shown for Reaction (2). The solid line shows the interaction energy for constrained optimizations with a fixed distance between the bonding carbon atoms in $\mathrm{C_{2h}}$ symmetry; the dotted line shows the interaction energy when the geometry of reactants is kept rigid. One can see that if the geometry relaxation were not taken into account for Reaction (2) the product well would be too shallow to provide the required minimum in the number of states even at low energies.

For computational reasons, the geometry optimizations for the present analysis were performed with the UB3LYP/DZ method. One might question the appropriateness of this method for geometry optimizations in a radical radical reaction. In Fig. 1 the interaction energy [CASPT2(10e,10o)/cc-pvdz] for the geometry optimized with the UB3LYP/cc-pvdz method (solid line) in the $\mathrm{C_{2h}}$ symmetry configuration is compared with the one for the geometry optimized with the CASPT2(6e,6o)/cc-pvdz method (dashed-dotted line) for Reaction (2). This comparison demonstrates an excellent agreement between the two methods. All UB3LYP calculations have been performed using the GAUSSIAN program package [13].

The effect of the basis set on the calculated interaction energy for Reaction (3) is shown in Fig. 2.

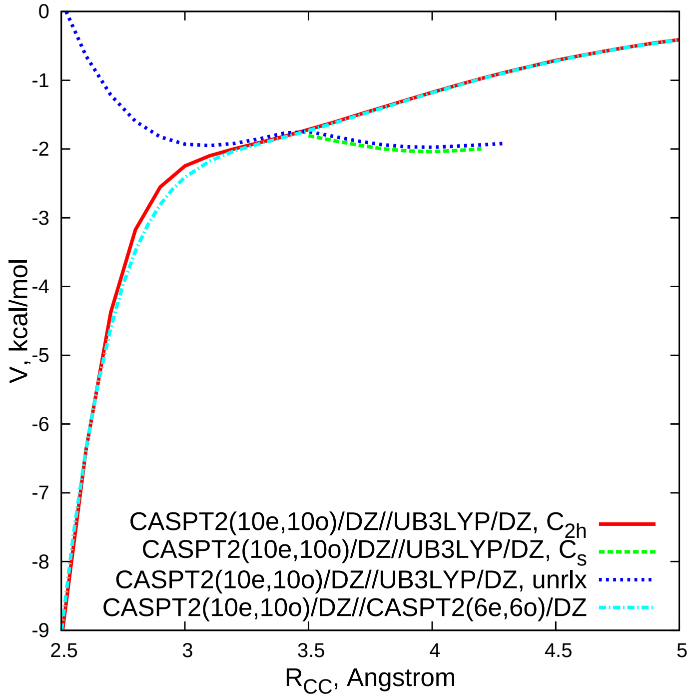

Figure 1: The CASPT2(10e,10o)/cc-pvdz interaction energy for Reaction (2) along the minimum energy path for different optimization methods. The solid (red) line corresponds to the UB3LYP/cc-pvdz method in $\mathrm{C_{2h}}$ symmetry. The dashed (green) line corresponds to the same method in $\mathrm{C_s}$ symmetry. For the dotted (blue) line no optimization has been used. The dashed-dotted (aqua) line corresponds to the CASPT2(6e,6o)/cc-pvdz method in $\mathrm{C_{2h}}$ symmetry.

In this figure the optimized energy in $\mathrm{C_s}$ symmetry is shown as a function of the distance between the two bonding carbon atoms. The optimization is performed using the UB3LYP/cc-pvdz method, with the subsequent single-point CASPT2(10e,10o) calculations performed with cc-pvdz, aug-cc-pvdz, and aug-cc-pvtz basis sets. One can see that while for the aug-cc-pvdz basis set the potential is 20-25 % more attractive in the kinetically important region between 2.5 and 5 Å, the aug-cc-pvtz basis set usage reduces this difference to about 10 % or less. One can expect that further basis-set increases will make this difference even smaller. Similar results are observed for Reactions (2) and (4). Therefore, we have decided to use the results of the CASPT2/cc-pvdz calculations as they are without any correction.

The exit channel, Reaction (5), has been discussed earlier [5]. In the current calculation we have used the same potential as in our previous work which uses the CASPT2(2e,2o)/cc-pvdz method for the orientational dependence of the potential together with a CI+1+2+QC/aug-cc-pvtz orientationally independent correction from the reference system $\mathrm{CH_3 + H}$. In Fig. 3 the energy profiles calculated along the minimum energy path (constrained optimization at a fixed distace between the radical carbon atom of phenyl and the hydrogen atom) for Reaction (5) are compared using different methods. For the solid (red), dashed (green), and dotted (blue) lines, the CASPT2(2e,2o)/cc-pvdz method was used for optimization with the subsequent CASPT2(2e,2o) calculation with cc-pvdz, aug-cc-pvdz, and aug-cc-pvtz basis sets, correspondingly. The dashed-dotted (yellow) line corresponds to the CASPT2(2e,2o)/aug-cc-pvdz optimization. For the dotted (magenta) and dashed-dotted (aqua) lines no optimization was used. The last result was obtained with the large (8e,8o) active space. One can see that the effects of the geometry relaxation on the potential as

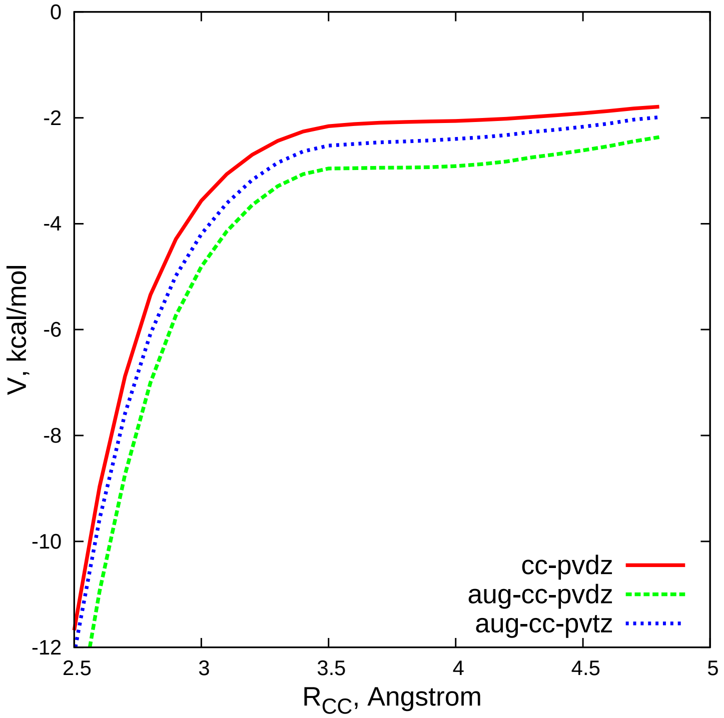

Figure 2: The interaction energy calculated with different basis sets along the minimum energy path for Reaction (3).

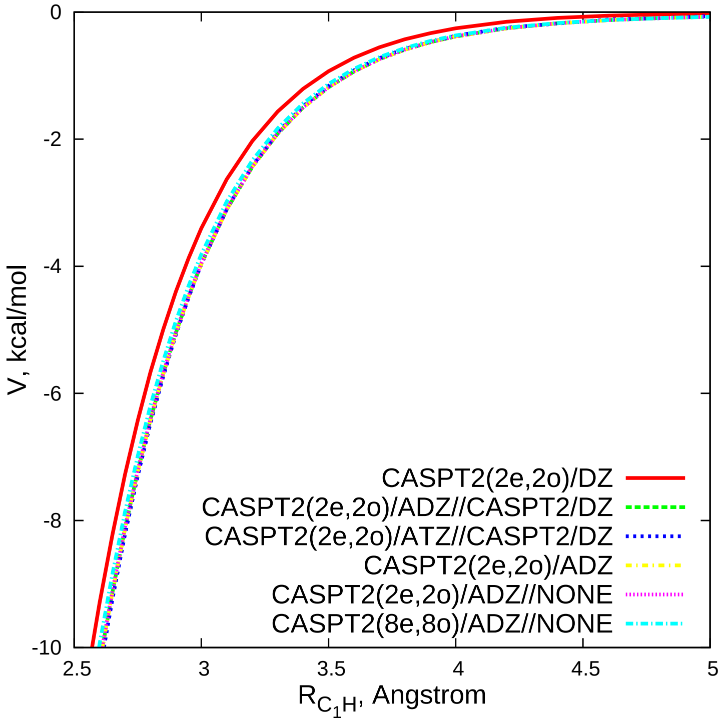

Figure 3: The interaction energy for Reaction (5) obtained with different methods as a function of the distance between the bonding carbon and hydrogen atoms in $\mathrm{C_{2v}}$ symmetry.

well as the increase of the active space in the CASSCF calculation are kinetically negligible. The only kinetically important effect on the potential is related to adding the diffuse functions to the cc-pvdz basis set. We have performed a small test calculation of the rate constant of the association reaction $\mathrm{C_6H_5 + H \rightarrow C_6H_6}$ using the CASPT2(2e,2o)/aug-cc-pvdz method which gave within the uncertainty of 5 % the same rate constant as our main method, CASPT2(2e,2o)/cc-pvdz with one-dimensional correction, in the 300-2500 K temperature range.

2.2 VRC-TST for multi-channel reactions

A detailed discussion of the application of variable reaction coordinate transition state theory to multi-channel reactions has been given elsewhere [3, 5]. For the present purposes it is useful to consider briefly the concept of a multifaceted divding surface, which is instrumental for understanding the application of the theory to the current problem.

Within the variable reaction coordinate approach a simple single-faceted dividing surface is defined in terms of a fixed distance between two pivot points, each of which is associated with a single reactant and is fixed in its reference frame for a given surface [1, 2]. For different surfaces, however, both the positions of the pivot points and the distance between them can be varied to minimize the reactive flux (number of states) for a given temperature or energy and angular momentum. Qualitatively a pair of pivot points can be associated with a specific channel along which the chemical reaction can proceed. In a general situation, when there are several reactive channels, multiple pivot points per reactant can be defined. In the resultant dividing surface, which we call multifaceted, each pair of the pivot points from different reactants is associated with a reactive channel. Some of these channels may become unavailable depending on the positions of the pivot points and the distances between them. By calculating the number of states for a given facet on an optimized multifaceted dividing surface one obtains an estimate for the rate constant through a reactive channel associated with that facet.

For the propargyl radical there are four ways in which it can react with another radical species. Therefore, we have used four pivot points for each reactant, two per each bonding carbon atom. Altogether this gives sixteen reactive channels, four identical channels for each of Reactions (2) and (4) and eight for Reaction (3). In principle, the position of the pivot point should be defined variationally. However, because the calculation of the number of states for a given facet is computationally very expensive (it typically required about 5000 potential samplings for kinetically important dividing surfaces) the reference association reaction,

$$\mathrm{C_3H_3 + H \rightarrow Products}, \tag{6}$$

has been used instead to find an optimal position of the pivot points of the propargyl radical. We have found that positioning the pivot points perpendicular to the propargyl plane at a distance of 1 bohr from the bonding carbon atom approximately minimizes the rate constant for Reaction (6) in the 500-2000 K temperature range. Therefore, we have used the same pivot point positions in our calculations. The distances between different pivot points in all pairs for a given dividing surface were set the same. Distances between the pivot points were chosen in the range between 3 and 10 bohr, which approximately correspond to the distances between the bonding carbon atoms being in the range between 5 and 12 bohr.

2.3 Master Equation Methodology

Application of the master equation (ME) to Reaction (1) has been discussed extensively in Refs. [7, 8]. For a general discussion the reader is also referred to Ref. [14]. In relation to the current calculation it is worth mentioning that the procedure described in the previous subsection allows one to obtain the energy and angular momentum resolved number of states for the so called "transitional" modes, which correlate with the rotations and relative translations of the fragments at infinite separation. In many situations knowing the number of states for the transitional modes is sufficient for the calculation of the rate constant for the corresponding association reaction [5]. For the ME application, however, one needs the total number of states for all non-reactive modes, which include the internal vibrational modes of the fragments also termed the conserved modes. To this end we assume that the vibrational frequencies of the fragments do not change significantly from their values at infinite separation of the fragments and convolve the number of states for the transitional modes with a direct sum over the quantized energy levels for the conserved modes in the harmonic approximation.

3 Results and Discussion

The energy profiles along the minimum energy paths for reactions (2)-(4) are shown in Fig. 4. The final energies were calculated with the CASPT2(10e,10o)/cc-pvdz method while the constrained geometry optimizations were performed at the UB3LYP/cc-pvdz level, as discussed in the previous section. In this figure the geometry optimizations for Reactions (2), (3), and (4) were constrained to C_{2h}, C_s, and C_{2h} symmetries, respectively. For Reactions (2) and (4) at smaller distances, when

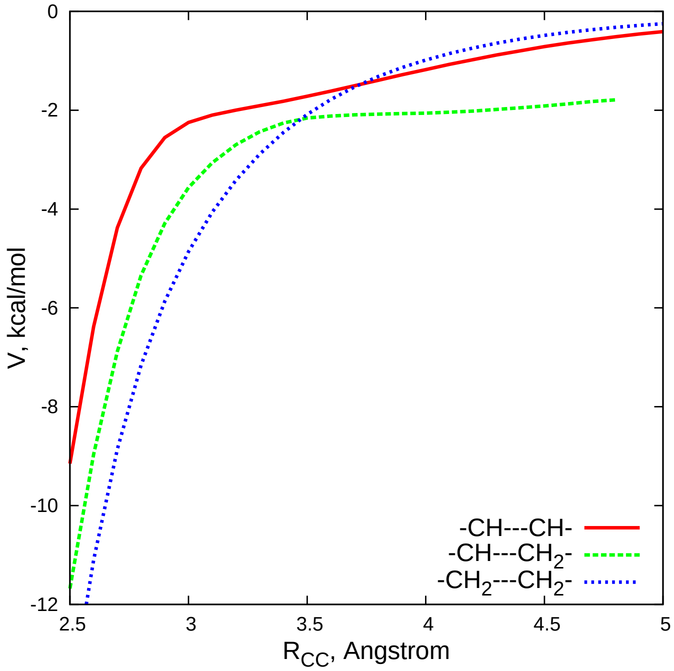

Figure 4: The interaction energies as functions of the distances between the bonding carbon atoms for Reactions (2)-(4).

the chemical bond between two carbon atoms starts forming, the C_{2h} symmetry seems to describe to the true (constrained) minima. For Reaction (2), however, at 3.5 angström the C_{2h} minimum bifurcates into two equivalent van der Waals configurations, which have lower C_s symmetry [cf. Fig. 1]. In these van der Waals configurations the CH group of one propargyl radical points to the π-bond of the second radical. A similar van der Waals configuration is formed for Reaction (3) at large separations between the bonding carbon atoms.

In the region in which the chemical bond between two carbon atoms is formed, $R_{CC} < 3.5$ Angström, and which is most important at combustion temperatures, the strongest attraction corresponds to Reaction (4). The reason for this is related to the fact that the two resonance electronic structures of the propargyl radical are not equivalent and the radical orbital is mostly localized on the CH_2 side of the radical. As a result, the interaction between the two CH_2 groups is strongest. The next strongest interaction is between the CH_2 and CH groups, Reaction (3), and the weakest interaction is the one between the two CH groups, cf. Fig. 4.

The rate constants for the association reactions (2)-(4), which were calculated using the VRC-TST approach, are shown in Fig. 5. As one might expect, the lowest rate constant corresponds

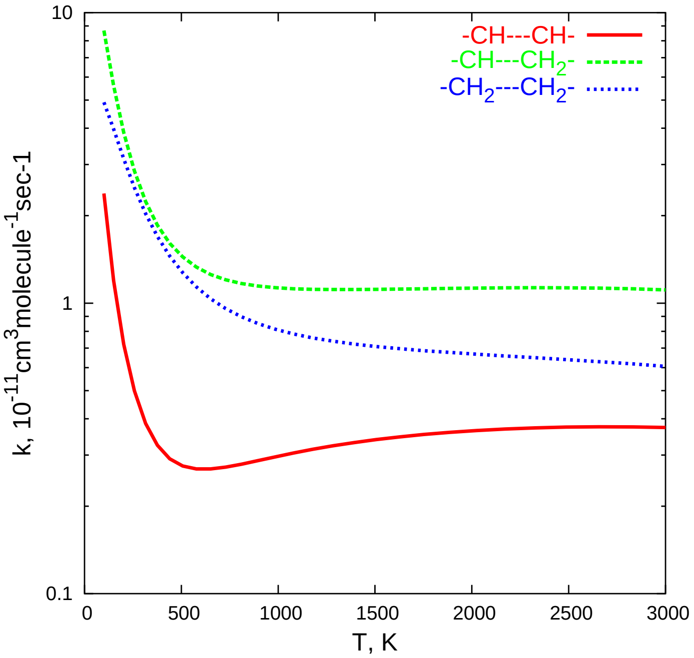

Figure 5: The VRC-TST rate constants for Reactions (2)-(4) as a function of temperature.

to Reaction (2), in accord with the fact that it proceeds on the least attractive reaction path, cf. Fig. 4. The largest rate constant corresponds to Reaction (3) even though the reaction path for this reaction is less attractive than the one for Reaction (4). This feature is related to the fact that there are twice as many reactive channels, 8, for Reaction (3) as for Reaction (4), 4 [see the discussion above about the application of VRC-TST to Reaction (1)]. Quantum mechanically one can say that the symmetry number for the transition state of Reaction (3) is 1 while for Reaction (4) it is 2. This gives an additional factor of two for the rate constant of Reaction (3) in comparison with Reaction (4).

As the temperature goes below 500 K the association rates of Reactions (2)-(4) show an inverse temperature behavior and start to grow. Similar behavior has been observed for reactions between large alkyl radicals [6]. This feature can be explained by the steric repulsion between the reactants while they are trying to form an energetically favorable configuration for the reaction to proceed. At low temperatures the main contribution to the rate constant comes from the dividing surfaces with relatively large separations between the reactants, which belong to the van der Waals region in the potential. The attractive part of the potential in that region is relatively flat. At the same time the propargyl radical is rather bulky. As a result at low, but not too low, temperatures only a fraction of the energetically favorable configurations make a significant contribution to the reactive flux through the dividing surface. Other configurations correspond to "bumping" reactants into each other and are strongly repulsive. As the temperature goes down and the separation between the reactants is increased, this fraction of energetically favorable configurations becomes larger. One can anticipate that at very low temperatures the steric repulsion will eventually play no role and the rate constant will reach a limit that is controlled by the long-range interactions [15], at which the rate constant is of the order of few $10^{-10}\ \mathrm{cm^3 molecule^{-1} s^{-1}}$.

Our results indicate that at room temperature Reactions (3) and (4) make comparable contributions of 48% and 44% to the total rate of the recombination reaction of two propargyl radicals, Reaction (1), while the contribution from Reaction (2) is only about 8%. These findings are in qualitative agreement with the experimental results of Fahr and Nayak [16], who reported the relative contributions from Reactions (2)-(4) to the total recombination rate to be about 15%, 25%, and 60%, correspondingly. The quantitative differences might be explained by the fact that at room temperature the optimal dividing surfaces correspond to relatively large separations between the reactants. In this situation it can be difficult for transition state theory to separate the different reactive channels and classical trajectory calculations should be used instead. Alternatively, these discrepancies may be related to experimental errors.

Figure 6 shows a comparison of the present predictions with the available experimental results [16–25] for the total rate constant of Reaction (1) at various temperatures and pressures. The rate constant was obtained using the master equation approach. The agreement between theory and experiment is excellent. In our previous work(see Fig. 11 of Ref. [8]), we used an analyical function for the association potential and chose the parameters in the function to get agreement with the experimental result at room temperature. This appeared at the time to be an adequate description of the association rate coefficients - it automatically predicted the rate coefficient obtained by Alkemade and Homann at slightly higher temperatures. However, subsequent experiments clearly indicated that our rate coefficients were consistently too large. The results of the present analysis, with $k_{P=\infty}$ decreasing with increasing temperature rather than increasing with T, largely resolve this discrepancy.

4 Concluding Remarks

We have demonstrated that variable reaction coordinate transition state theory in conjunction with the state-of-the-art electronic structure methods and the master equation methodology allows one to predict the rate coefficients of reactions with resonance stabilized radicals with quantitative accuracy.

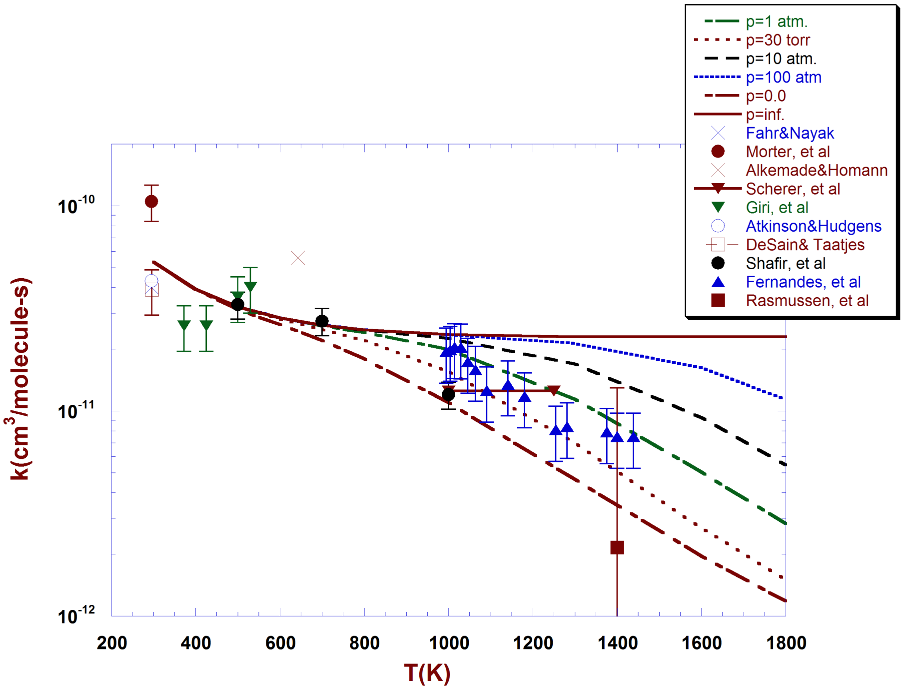

Figure 6: The total rate constant of Reaction (1) as a function of temperature at 0, 30, 760, 7600, and 76000 Torr pressures. The available experimental data are also shown.

Acknowledgments

This work was supported by the U. S. Department of Energy, Office of Basic Energy Sciences, Division of Chemical Sciences, Geosciences, and Biosciences. Sandia is a multiprogram laboratory operated by Sandia Corporation, a Lockheed Martin Company, for the United States Department of Energy under contract DE-AC04-94-AL85000. The work at Argonne was supported under DOE Contract Number DE-AC02-06CH11357.

References

[1] S. J. Klippenstein. *J. Chem. Phys.*, 94 (1991) 6469.

[2] S. J. Klippenstein. *J. Chem. Phys.*, 96 (1992) 367.

[3] Y. Georgievskii and S. J. Klippenstein. *J. Phys. Chem. A*, 107 (2003) 9776.

[4] Y. Georgievskii and S. J. Klippenstein. *J. Chem. Phys.*, 118 (2003) 5442.

[5] L. B. Harding, Y. Georgievskii, and S. J. Klippenstein. *J. Phys. Chem. A*, 109 (2005) 4646.

[6] S. J. Klippenstein, Y. Georgievskii, and L. B. Harding. *Phys. Chem. Chem. Phys.*, 8 (2006) 1133.

[7] J. A. Miller and S. J. Klippenstein. *J. Phys. Chem. A*, 105 (2001) 7254.

[8] J. A. Miller and S. J. Klippenstein. *J. Phys. Chem. A*, 107 (2003) 7783.

[9] J. A. Miller and C. F. Melius. *Combust. Flame*, 91 (1992) 21.

[10] C. F. Melius, J. A. Miller, and E. M. Evleth. *Proc. Combust. Inst.*, 24 (1992) 621.

[11] H.-J. Werner, P. J. Knowles, R. Lindh, M. Schütz, T. Korona P. Celani, F. R. Manby, G. Rauhut, R. D. Amos, A. Bernhardsson, A. Berning, D. L. Cooper, M. J. O. Deegan, A. J. Dobbyn, F. Eckert, C. Hampel, G. Hetzer, A. W. Lloyd, S. J. McNicholas, W. Meyer, M. E. Mura, A. Nicklass, P. Palmieri, R. Pitzer, U. Schumann, H. Stoll, A. J. Stone, R. Tarroni, and T. Thorsteinsson. Molpro, version 2002.10, a package of *ab initio* programs.

[12] P. Celani and H.-J. Werner. *J. Chem. Phys.*, 112 (2000) 5546.

[13] M. J. Frisch, G. W. Trucks, H. B. Schlegel, G. E. Scuseria, M. A. Robb, J. R. Cheeseman, V. G. Zakrzewski, J. A. Montgomery, R. E. Stratmann, J. C. Burant, S. Dapprich, J. M. Millam, A. D. Daniels, K. N. Kudin, M. C. Strain, O. Farkas, J. Tomasi, V. Barone, M. Cossi, R. Cammi, B. Mennucci, C. Pomelli, C. Adamo, S. Clifford, J. Ochterski, G. A. Petersson, P. Y. Ayala, Q. Cui, K. Morokuma, D. K. Malick, A. D. Rabuck, K. Raghavachari, J. B. Foresman, J. Cioslowski, J. V. Ortiz, B. B. Stefanov, G. Liu, A. Liashenko, P. Piskorz, I. Komaromi, R. Gomperts, R. L. Martin, D. J. Fox, T. Keith, M. A. Al-Laham, C. Y. Peng, A. Nanyakkara, C. Gonzalez, M. Challacombe, P. M. W. Gill, B. Johnson, W. Chen, M. W. Wong, J. L. Andres, C. Gonzalez, M. Head-Gordon, E. S. Replogle, and J. A. Pople. *Gaussian 98.* Gaussian Inc., Pittsburgh, PA, 1998.

[14] J. A. Miller and S. J. Klippenstein. *J. Phys. Chem. A*, 110 (2006) 10528.

[15] Y. Georgievskii and S. J. Klippenstein. *J. Chem. Phys.*, 122 (2005) 194103.

[16] A. Fahr and A. Nayak. *Int. J. Chem. Kinet.*, 32 (2000) 118.

[17] U. Alkemade and K. H. Homann. *Z. Phys. Chem. Neue Folge*, 161 (1989) 19.

[18] S. Scherer, Th. Just, and P. Frank. *Proc. Combust. Inst.*, 28 (2000) 1511.

[19] D. B. Atkinson and J. W. Hudgens. *J. Phys. Chem. A*, 103 (1999) 4242.

[20] C. L. Morter, S. K. Farhat, J. D. Adamson, G. P. Glass, and R. F. Curl. *J. Phys. Chem.*, 98 (1994) 7029.

[21] J. D. DeSain and C. A. Taatjes. *J. Phys. Chem. A*, 107 (2003) 4843.

[22] B. R. Giri, H. Hippler, M. Olzmann, and A. N. Unterreiner. *Phys. Chem. Chem. Phys.*, 5 (2003) 4641.

[23] E. V. Shafir, I. R. Slagle, and V. D. Knyazev. *J. Phys. Chem. A*, 107 (2003) 8893.

[24] C. L. Rasmussen, M. S. Skjøth-Rasmussen, A. D. Jensen, and P. Glarborg. *Proc. Combust. Inst.*, 30 (2005) 1023.

[25] R. X. Fernandes, H. Hippler, and M. Olzmann. *Proc. Combust. Inst.*, 30 (2005) 1033.